Elevated Intraocular Pressure Causes Inner Retinal Dysfunction Before Cell Loss in a Mouse Model of Experimental Glaucoma

Benjamin J. Frankfort,[1] *A. Kareem Khan,*[1,2] *Dennis Y. Tse,*[1,2] *Inyoung Chung,*[1,3] *Ji-Jie Pang,*[1] *Zhuo Yang,*[1] *Ronald L. Gross,*[1] *and Samuel M. Wu*[1]

Purpose. We assessed the relationship among intraocular pressure (IOP), histology, and retinal function changes in a mouse model of induced, chronic, mild ocular hypertension.

Methods. IOP was elevated experimentally via anterior chamber injection of polystyrene beads and measured twice weekly with a rebound tonometer. Histology was assessed with a combination of neurobiotin (NB) retrograde labeling of retinal ganglion cells (RGCs) and TO-PRO3 staining. Retinal function was assessed with serial dark-adapted electroretinograms (ERGs) optimized for detection of the a-wave, b-wave, and positive and negative scotopic threshold responses (pSTR, nSTR). Comparisons between bead-injected and saline-injected (control) eyes were conducted.

Results. IOP remained elevated for at least 3 months following a single injection of polystyrene beads. Elevated IOP resulted in a mild, progressive reduction of RGCs, and a mild increase in axial length at 6 and 12 weeks after bead injection. The raw b-wave amplitude was increased shortly after IOP elevation, but the raw a-wave, pSTR, and nSTR amplitudes were unchanged. pSTR and nSTR amplitudes were normalized to the increased b-wave. With this normalization, the pSTR amplitude was decreased shortly after IOP elevation.

Conclusions. Polystyrene bead injection results in a mild, chronic elevation of IOP that recapitulates several critical aspects of human ocular hypertension and glaucoma, and results in early changes in retinal electrical function that precede histologic changes. It is possible that glaucoma associated with elevated IOP involves the early disruption of a complex combination of retinal synapses. (*Invest Ophthalmol Vis Sci.* 2013;54:762–770) DOI:10.1167/iovs.12-10581

From the [1]Cullen Eye Institute, Department of Ophthalmology, Baylor College of Medicine, Houston, Texas; and the [3]Department of Ophthalmology, Gyeongsang National University, Jinju, Republic of Korea.

[2]These authors contributed equally to the work presented here and should therefore be regarded as equivalent authors.

Support for this work was provided by National Institutes of Health Grants EY019908, EY04446, and EY02520 (SMW), and EY021479 (BJF); Retina Research Foundation Pilot Study grants (Houston, Texas; BJF and SMW); Research to Prevent Blindness, Inc. (New York, New York; BJF and SMW); and an International Retinal Research Foundation Loris and David Rich Award (Birmingham, Alabama; DYT). The authors alone are responsible for the content and writing of the paper.

Submitted for publication July 12, 2012; revised October 16 and December 1, 2012; accepted December 2, 2012.

Disclosure: **B.J. Frankfort**, None; **A.K. Khan**, None; **D.Y. Tse**, None; **I. Chung**, None; **J.-J. Pang**, None; **Z. Yang**, None; **R.L. Gross**, None; **S.M. Wu**, None

Corresponding author: Benjamin J. Frankfort, Cullen Eye Institute, Department of Ophthalmology, Baylor College of Medicine, Houston, TX, 77030; benjamin.frankfort@bcm.edu.

Glaucoma is the second leading cause of blindness worldwide and is defined by characteristic abnormalities of the optic nerve associated with retinal ganglion cell (RGC) death, and specific changes in retinal sensitivity and perimetric testing.[1] These changes include an early mild diffuse loss of retinal contrast sensitivity and a later denser focal loss in classic patterns.[2–5] However, the details of the early RGC dysfunction that presumably underlie the initial mild diffuse loss are not well understood.

Elevated IOP is the most significant single risk factor for the development and progression of glaucoma, and to our knowledge is the only modifiable risk factor thus far identified conclusively.[6–8] Extremely high IOP results in rapid and profound vision loss associated with severe optic nerve damage. Ocular hypertension, defined as a chronic, mild elevation of IOP, can lead to slowly progressive changes in visual function and optic nerve appearance.[7] To investigate the role of IOP on the optic nerve and RGCs, and to study mechanisms of glaucomatous damage, various rodent models of experimental glaucoma have been generated.[9–19] Most recently, an experimental rodent model of ocular hypertension and glaucoma based on the injection of microspheres into the anterior chamber was developed.[19] This "microbead occlusion model" has been reproduced with minor modifications by several labs, and is characterized by a mild IOP elevation with low variability, as well as various degrees of neurodegeneration.[15,16] Interestingly, this neurodegeneration appears to follow a sequential retrograde pattern, progressing from abnormal axon transport to axon degeneration to cell body loss over a period of several weeks to months.[15,19,20] While there is general agreement of the basic characteristics of this model, some variability in the amount of neurodegeneration has been reported, and a species-dependent component of RGC loss has been observed.[15–17,19] For all published rodent models of experimental ocular hypertension the majority of studies have focused on anatomic, histopathologic, and immunohistochemical analyses of overall retinal appearance, RGC survival, and axon changes. A much smaller number of publications have focused on changes in retinal physiology. In general, these physiology-based studies have been conducted on animals with significant IOP increase and/or RGC loss, which may limit their applicability to the more common human condition of chronic, mild IOP elevation.[13,21–28]

The electroretinogram (ERG) is a well-established tool for uncovering the gross physiologic state of the living, intact retina. Its core components, the a-wave (which represents first-order neurons/photoreceptor signaling) and the b-wave

(which represents mostly second-order neurons/bipolar cell signaling), are well understood. Other components have been identified that represent signaling from other retinal neurons. Two such components, the positive and negative scotopic threshold responses (pSTR and nSTR) likely represent inner retinal signaling from third order neurons, the RGCs and AII amacrine cells, respectively.[29–31]

We have used minor modifications to one version of the microbead occlusion model in mice to achieve a chronic, mild IOP elevation that resembles the IOP elevation seen typically in human ocular hypertension and early glaucoma.[16] We then performed histologic analysis as well as serial ERGs over a 12-week period. We report a mild loss of RGCs over time that is consistent with published results. Interestingly, we detected changes in several components of the dark-adapted ERG by two to four weeks after IOP elevation, which precede RGC loss and do not correlate with RGC loss. These changes in retinal function occurred in a manner that is related to cumulative IOP exposure. The speed at which these changes occurred implies an effect of experimental IOP elevation on retinal function that is distinct from the sequential pattern of axonal dysfunction that has been reported previously.

Materials and Methods

Induction of Ocular Hypertension/Experimental Glaucoma

Six-week-old C57Bl/6 female mice were purchased from Jackson Laboratories (Bar Harbor, ME) and treated in accordance NIH guidelines, the ARVO Statement for the Use of Animals in Ophthalmic and Vision Research, and the Baylor College of Medicine IACUC welfare guidelines. To elevate IOP experimentally, animals first were anesthetized with a weight-based intraperitoneal injection of ketamine (80 mg/kg), xylazine (16 mg/kg), and acepromazine (1.2 mg/kg). A drop each of 0.5% proparacaine hydrochloride and 1% tropicamide then was applied to the left eye. A 30-gauge needle was used to puncture the midperipheral cornea. A pulled glass micropipette with an inner diameter of 75 μm attached to a Hamilton syringe was inserted into the anterior chamber through the corneal incision and advanced to the center of the pupil. Care was taken not to touch the lens or the posterior surface of the cornea at any point. The dilated pupil allowed for better visualization of anterior chamber depth and also prevented externalization of iris tissue during the procedure. A mixture of approximately 4.7×10^6 of 6 μm diameter blue polystyrene beads and 2.4×10^7 of 1 μm diameter yellow polystyrene beads in a total volume of 1 to 2 μL (Polysciences, Inc., Warrington, PA), followed by 3 μL of sodium hyaluronate (Provisc; Alcon Laboratories, Ft. Worth, TX) then was injected into the anterior chamber over a period of approximately 90 seconds.[16] The sodium hyaluronate served to "push" the beads into the anterior chamber angle, as well as prevent reflux of beads during and after the procedure. To confirm the basic ERG findings, red or yellow 6 μm diameter beads were injected instead of blue beads. After the procedure, all eyes were treated with a drop of 0.5% moxifloxacin. The right eye was left uninjected in all animals to serve as a control. Additional controls were performed by replacing the beads with 1× PBS (saline) and treating the left eye of additional animals as above.

Measurement of Intraocular Pressure

Animals were kept in a holding room maintained at 68° to 72° with a light-dark cycle of 12 hours light and 12 hours dark. For all animals, IOP was measured with a rebound tonometer (Tonolab; Icare, Espoo, Finland) before treatment and twice weekly in both eyes for 6 weeks in all animals ($N = 107$) and for 12 weeks in a subset of animals ($N = 37$).[32] To minimize variability, all IOP readings were taken at the same time of day (beginning at 9 AM), on the same days of the week (Tuesday and Friday), and cages were tested in the same order at each session. Before measurement, the animals were anesthetized briefly with inhaled isoflurane so that they did not require restraint during measurement. Animals were placed on their stomachs and the IOP reading obtained from the central cornea of each eye. The tonometer (Tonolab; Icare) reports as the IOP an average of 3 measurements. The average of at least 2 such readings (6 measurements) was considered to be the IOP. The cumulative IOP difference for each animal was calculated according to the following equation:

$$Cumulative\ IOP\ difference(mmHg) = \sum (IOP_{injected} - IOP_{uninjected})_n \quad (1)$$

where n = the number of IOP measurements taken per animal (13 for animals followed for 6 weeks and 25 for animals followed for 12 weeks).

Immunohistochemistry/Cell Counting

Neurobiotin (NB) labeling was performed according to the protocol of Pang and Wu except that the eyeballs were dissected under ambient light rather than infrared conditions.[33] After labeling, eyes were whole-mounted, fixed, and counterstained with the fluorescent nuclear marker TO-PRO3. Images were acquired with a laser confocal microscope (LSM 510; Carl Zeiss, Oberkochen, Germany) and processed with Zeiss LSM-PC software (Carl Zeiss). Four regions equidistant between the optic nerve and the peripheral retina as well as four additional regions equidistant between the first four regions and the peripheral retina were imaged from each eye. The identity of these regions was masked, and NB-positive cells were counted manually from all eight regions by a single investigator, assisted by ImageJ software (available online at http://rsbweb.nih.gov/ij/, provided in the public domain by National Institutes of Health, Bethesda, MD). TO-PRO3–positive cells were counted by a different investigator in a subset of retinas. This investigator also counted NB-positive cells to verify the results of the first investigator. Each region had an area of 0.053 mm^2 and this was used to convert cell counts into the cells/mm^2. Cy3-conjugated secondary antibody was used at a dilution of 1:200 (Jackson ImmunoResearch, West Grove, PA). TO-PRO3 was used together with secondary antibodies at a dilution of 1:3000 (Molecular Probes, Eugene, OR).

Measurement of Eye Size

The optic nerves of freshly enucleated eyes were trimmed flush with the posterior sclera. Eyes then were placed cornea down on a cover slip, and axial length measured with micro camera and controller system (LS-7601 Digital Micrometer; Keyence Corp., Elmwood Park, NJ). Measurements were made constantly as the eye was manipulated into position and the largest number was recorded as the axial length. The eye then was rotated 90° along the anterior–posterior axis and the measurements repeated. The average of these two measurements was considered to be the axial length of the eye.

ERG Recordings

Before testing, mice were allowed to adapt to the dark for a minimum of 2 hours. Under dim red light, mice were prepared for ERG testing as described previously.[29] Signals were amplified with a Grass P122 amplifier, bandpass 0.1 to 1000 Hz (Grass Instruments, West Warwick, RI). Data were acquired with a National Instruments data acquisition board at a sampling rate of 10,000 Hz. Traces were analyzed with custom software written in Matlab (MathWorks, Natick, MA).

Scotopic flashes were generated with cyan light emitting diodes calibrated with a photometer and converted to the unit photoisomerizations/rod, where 1 scot cd m^2 = 581 photoisomerizations/rod/s.[29,31,34] A 5 ms stimulus of 500 nm wavelength light was used for all flashes. To remove oscillatory potentials before fitting, the scotopic b-wave was filtered digitally using the filtfilt function in Mathlab (low-pass filter, Fc =

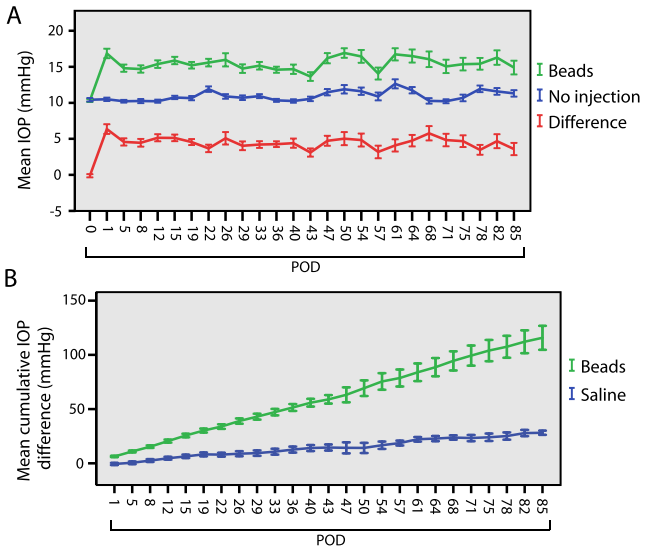

Figure 1. Patterns of IOP. IOP is elevated in bead-injected eyes. (**A**) Mean IOP for bead-injected (*green*) and uninjected (*blue*) eyes as measured twice weekly over 12 weeks ($N = 96$ animals through postoperative day [POD] 43, $N = 33$ from PODs 47–85, see Table 1). IOP is elevated by POD 1 and remains elevated at every measured time point for at least 12 weeks (*t*-test, $P < 0.05$). The difference in IOP between bead-injected and uninjected eyes is presented in *red*. (**B**) Mean cumulative IOP difference between bead-injected and saline-injected eyes. The cumulative IOP difference for each animal was determined according to Equation 1 (see Materials and Methods) and used to calculate the mean cumulative IOP difference (mm Hg). Bead-injected eyes are subject to a larger final cumulative IOP than saline-injected eyes at all measured time points (*t*-test, $P < 0.01$). *Error bars* represent one SEM for panels.

60 Hz; MathWorks). The pSTR and nSTR responses were measured under the stimuli strength described previously.[29] Stimulus strength in this report is defined according to a log intensity scale, where $\log 10^0 = 1$ photoisomerization/rod.

To assist with intra-animal ERG analysis, the "b-wave amplitude ratio" and the analogous "a-wave amplitude ratio" were determined for each animal according to the following equation:

$$b\text{-}wave\ amplitude\ ratio = \frac{mean\ b\text{-}wave_{injected}}{mean\ b\text{-}wave_{uninjected}} \quad (2)$$

where the mean b-wave was obtained from the average of the b-wave amplitudes obtained at six different subsaturation stimuli ranging on the log intensity scale from –0.217 to 2.30 ($0.6–2 \times 10^2$ photoisomerizations/rod). Amplitudes of the a-wave were obtained at the same six subsaturation stimuli. STR measurements for injected eyes (bead or saline) were obtained at two stimuli of log intensity –2.09 and –1.25 (8×10^{-3} and 5.5×10^{-2} photoisomerizations/rod). These stimuli were chosen because they allowed for reliable measurements of STR amplitudes and were definitely independent from the b-wave.[29] These measurements were averaged, and then normalized to the uninjected eye of the same animal according to the b-wave amplitude ratio (Equation 2) such that:

$$normalized\ STR_{injected} = \frac{STR_{injected}}{b\text{-}wave\ amplitude\ ratio} \quad (3)$$

This then was converted into the STR difference according to the following equation:

$$STR\ difference = normalized\ STR_{injected} - STR_{uninjected} \quad (4)$$

The use of these equations allowed for the comparison of the STR/b-wave ratio while reducing intra-animal variability.

Statistical Analysis

All analyses were performed using SPSS Version 20 (IBM, Armonk, NY). ERG measurements obtained at individual light stimuli across multiple time points were analyzed with a repeated measured ANOVA to compare between groups. Stronger relationships were explored with an independent samples *t*-test at specific time points. Confirmatory analysis of averaged data was performed in the same fashion and used for data presentation. An independent samples *t*-test was used for all other analyses.

Results

Injection of Polystyrene Beads Results in IOP Elevation

The left eyes of 96 six-week old female C57Bl/6 mice received a single transcorneal intracameral injection of polystyrene beads followed by sodium hyaluronate in a single syringe (see Materials and Methods).[16] The right eye of each animal remained uninjected to serve as an intra-animal control. An additional 11 animals had left eye sham injections of saline instead of beads (see Materials and Methods). The mean IOP of bead-injected eyes was higher than that of uninjected eyes at every time point over the entire 12-week study period (*t*-test, $P < 0.05$ for each point, Fig. 1A). The mean IOP for bead-injected, saline-injected, and uninjected eyes were 15.3, 12.4, and 10.8 mm Hg, respectively (Table 1). The mean IOP difference between bead-injected and uninjected eyes was 4.5 mm Hg (41.7% increase) and remained relatively constant throughout the study (Fig. 1A, Table 1). Severe IOP spikes were rare among bead-injected eyes, occurring in only 1.8% of all IOP measurements (29/1644, Table 1). To approximate the amount of additional IOP exposure experienced by injected

Table 1. Patterns of IOP Change in Experimental Eyes

Treatment	*N*	Mean IOP, mm Hg (SD)	Mean IOP Difference, mm Hg (SD)	% IOP Spikes
Beads, 6 wk	63	15.0 (5.6)	4.6 (5.3)	1.2
Beads, 12 wk	33	15.6 (5.5)	4.4 (5.6)	2.3
Beads, all	96	15.3 (5.6)	4.5 (5.4)	1.8
Saline, 6 wk	7	12.5 (2.6)	1.2 (2.3)	0
Saline, 12 wk	4	12.3 (3.3)	1.0 (2.6)	0
Saline, all	11	12.4 (2.9)	1.1 (2.5)	0
No injection, 6 wk	70	10.5 (2.3)		0
No injection, 12 wk	37	11.2 (3.1)		0
No injection, all	107	10.8 (2.7)		0

Animals with 6 weeks and 12 weeks of follow-up are presented separately and then pooled (all). IOP was measured twice weekly for all eyes beginning on POD 1 and continuing until POD 43 (6 weeks) or POD 85 (12 weeks). The mean IOP and mean IOP difference were similar regardless of the duration of study. IOP spikes (IOP $\geq$ 30 mm Hg) were uncommon in bead-injected eyes and never seen in saline-injected or uninjected eyes.

Table 2. Mean Cumulative IOP Difference in Experimental Eyes

Treatment	*N*	Mean Cumulative IOP Difference, mm Hg (SD)
Beads, 6 wk	96	59.0 (38.2)
Beads, 12 wk	33	115.7 (63.4)
Saline, 6 wk	11	14.6 (9.4)
Saline, 12 wk	4	28.2 (3.8)

Bead-injected eyes were exposed to a much greater cumulative IOP than saline-injected eyes (*t*-test, $P < 0.01$ at all time points). Cumulative IOP difference (mm Hg) for each animal was calculated according to Equation 1.

eyes compared to uninjected eyes, we calculated the cumulative IOP difference for all bead-injected and saline-injected eyes (Equation 1). Bead-injected eyes were exposed to a much greater cumulative IOP difference than saline-injected eyes (*t*-test, $P < 0.01$, Fig. 1B, Table 2). Thus, similar to human ocular hypertension and chronic glaucoma, bead injection resulted in a mild IOP elevation with a low incidence of IOP spikes and an increased cumulative IOP exposure.

Injection of Polystyrene Beads Results in a Mild Loss of RGCs

To determine if bead injection resulted in a loss of RGCs, we performed retrograde labeling of RGC axons with NB in freshly enucleated eyes (see Materials and Methods). NB is a well-established intracellular label, which traverses gap junctions and reliably labels RGCs.[33] To help determine cell boundaries and also to allow for the counting of amacrine cells, we counterstained retinas with TO-PRO3, which stains nucleic acids. We counted eight retinal regions from flat mounts of injected and uninjected eyes of the same animal at 6 and 12 weeks postinjection (Fig. 2). Gross RGC density and axon confluence were decreased in the periphery compared to the midretina as has been reported previously (Fig. 2, not shown).[33] We observed a gradual and mild reduction in RGC somas over time, with a 7.4% reduction at 6 weeks and an 11.2% reduction at 12 weeks (Table 3). The distribution of RGC reduction was similar in the periphery and midretina (not shown). We did not detect a substantial correlation between cumulative IOP difference and RGC loss at either time point (6 weeks, $r = -0.102$, $P = 0.83$; 12 weeks, $r = 0.081$, $P = 0.80$; Pearson's correlation). Despite a mild increase in IOP and cumulative IOP, saline-injected eyes did not have reduced numbers of RGCs (Table 3). To determine if numbers of other inner retinal neurons also were reduced, we counted cells that stained for TO-PRO3 but not NB, which represent amacrine cells.[33] We observed a very mild reduction of these cells (approximately 2%) in bead-injected eyes, which was not statistically significant ($N = 5$, not shown). Finally, we assessed

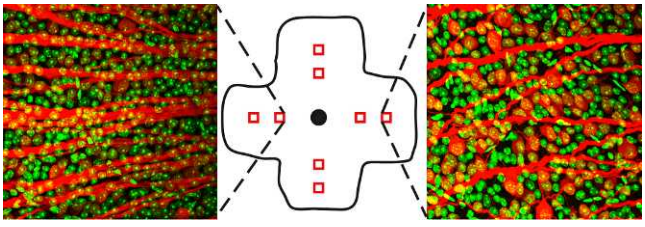

Figure 2. Inner retina staining. Neurobiotin-positive (*red*) and TO-PRO3–positive (*green*) cells were counted from 8 regions per retina (*middle, red squares*). *Left*: typical staining pattern from the midretina. *Right*: typical staining pattern from the peripheral retina.

Table 3. NB Staining in Experimental Eyes

Treatment	*N*	NB-Positive Cells/mm² (SD)
No injection, 6 wk	7	3790.6 (630.2)
No injection, 12 wk	16	3705.7 (647.2)
Beads, 6 wk	7	3500.0 (660.4)
Beads, 12 wk	12	3315.1 (749.1)
Saline, 12 wk	4	3817.0 (766.0)

NB-positive somas were counted at 6 and 12 weeks postinjection. RGC numbers were reduced by 7.4% in bead-injected eyes at 6 weeks postinjection and by 11.2% at 12 weeks postinjection when compared to uninjected eyes. These reductions were statistically significant (*t*-test, $P < 0.05$). Saline-injected eyes did not show reduced RGCs.

the thickness of the retina in cross-section and did not observe a difference in retinal thickness in either the outer or inner nuclear layer, suggesting that photoreceptors and bipolar cells were grossly intact (not shown).

Injection of Polystyrene Beads Results in an Increase in Axial Length

Others have reported an increase in axial length over time in mice with experimental glaucoma.[16,35] To determine if similar findings were present in our model, we measured the diameter of the globe in several axes with a laser micrometer at 6 and 12 weeks after bead-injection (see Materials and Methods). The axial length of bead-injected eyes was increased by 4.7% at 6 weeks postinjection and by 3.9% at 12 weeks postinjection (Table 4). Because the axial length increase essentially was stable after 6 weeks, this suggested that IOP-induced axial length elongation occurs early, and then remains constant with normal growth thereafter. Other measured axes were unchanged (not shown).

Injection of Polystyrene Beads Causes ERG Abnormalities in a Cumulative IOP-Dependent Manner

We chose a group of 30 animals (24 bead-injected and 6 saline-injected) for ERG study over time. Following bead or saline injection, these animals were examined with serial bilateral simultaneous full field flash ERGs at 2-week intervals, beginning at 2 weeks postinjection and continuing through 12 weeks postinjection. Four animals were excluded from the analysis because of early death, and one animal was excluded because of a deformed cornea, leaving a final study group of 25 animals (20 bead-injected and 5 saline-injected). In our study, baseline ERG results were assessed by comparing bead-injected, saline-injected, and uninjected eyes. Subsequent analyses of intra-animal changes in the ERG between bead-injected and uninjected eyes were conducted by comparison with intra-animal changes in the ERG between saline-injected and uninjected eyes. We evaluated the amplitudes of the pSTR, nSTR, b-wave, and a-

Table 4. Axial Length in Experimental Eyes

Time Postinjection	*N*	Bead-Injected Eyes, mm (SD)	Uninjected Fellow Eyes, mm (SD)
6 wk	10	3.14 (0.15)	3.00 (0.10)
12 wk	7	3.43 (0.20)	3.30 (0.12)

Axial lengths of freshly enucleated eyes were measured at 6 and 12 weeks postinjection. Axial length was increased by 4.7% at 6 weeks postinjection and by 3.9% at 12 weeks postinjection. These increases were statistically significant (*t*-test, $P < 0.05$).

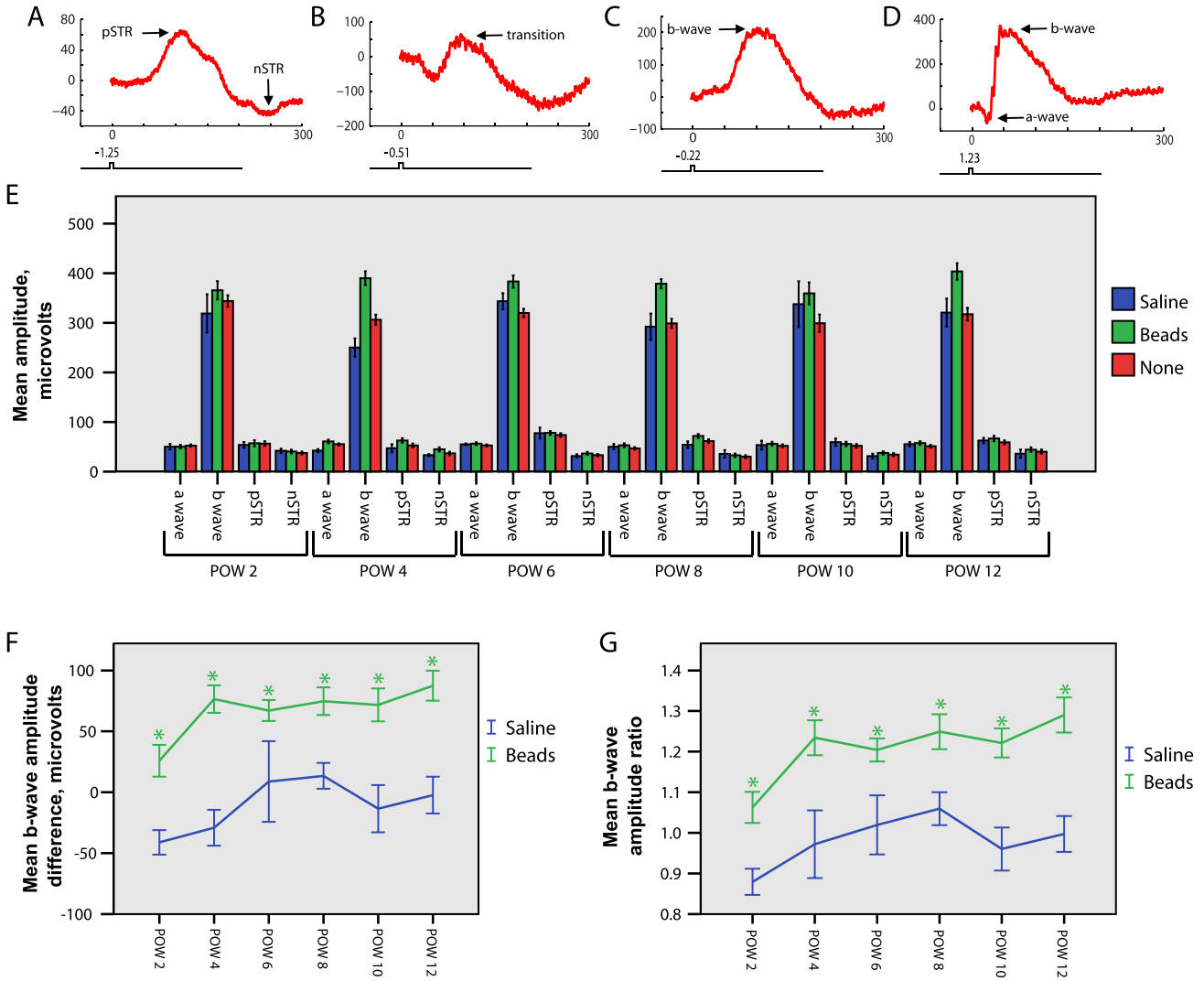

Figure 3. ERG analysis. IOP elevation results in b-wave abnormalities. (**A–G**). 20 bead-injected and 5 saline-injected animals were followed with sequential bilateral simultaneous ERGs (see Materials and Methods) at 2-week intervals beginning at 2 weeks postinjection and continuing for 12 weeks (postoperative weeks [POWs] 2–12). (**A–D**). Representative tracings at increasing light stimuli (log intensity scale, see Materials and Methods). For all tracings, the x-axis represents msec and the y-axis represents μV. Note the change in scale of the y-axis for each tracing to highlight best the individual waveforms. (**A**) At low scotopic range light intensities the pSTR and nSTR are observed. (**B**) At slightly greater light intensities a transition wave is detected. (**C**) At slightly greater light intensities the b-wave is first observed, and the pSTR and nSTR are no longer detected. (**D**) At brighter light intensities the a-wave and b-wave are detected. (**E**) Raw amplitudes of ERG waveforms obtained from bead-injected, saline-injected, and uninjected eyes. For the a-wave and b-waves, amplitudes obtained at six stimulus levels were compared for all stimuli and at all time points, and then averaged for presentation. For the pSTR and the nSTR, amplitudes obtained at two stimulus levels were compared for stimuli and at all time points, and then averaged for presentation (see text, Materials and Methods). The b-wave amplitude of bead-injected eyes is increased compared to either saline-injected or uninjected eyes, whereas the a-wave, pSTR, and nSTR amplitudes are unchanged (ANOVA $P < 0.001$). (**F**) The b-wave amplitude difference was calculated by subtracting the b-wave amplitude of the uninjected eye from the b-wave amplitude of the injected eye (beads or saline) for each animal at every time point. This difference is positive, indicating an increased b-wave amplitude in bead-injected eyes at all time points. (**G**) The b-wave amplitude ratio was calculated according to Equation 2 (see Materials and Methods). Bead-injected eyes have an increased mean b-wave amplitude ratio compared to saline-injected eyes at all time points. (**F, G**) suggest that the intra-animal b-wave amplitude is increased rapidly for bead-injected eyes at each time point (*t*-test, * = $P < 0.05$). *Error bars* represent one SEM for all panels.

wave. Because of synaptic convergence the sensitivity of light responses increases after every synapse from photoreceptors to the inner retina. Consequently, elements of the ERG are observable at different light intensities, with the high sensitivity pSTR and nSTR observable at the lowest intensities, followed by the b-wave and finally the a-wave (Figs. 3A–D).

We conducted our analysis across 10 distinct subsaturation stimuli (see Materials and Methods). At the two dimmest light stimuli (less than 0.1 photoisomerizations/rod), we consistently and reliably obtained pSTR and nSTR recordings that were distinct from the b-wave.[29] At the next two brightest light stimuli (between 0.1 and 0.3 photoisomerizations/rod), transitional waveforms including elements of the pSTR, nSTR, and b-wave were obtained. Therefore, these stimulus strengths were not used in the ERG analysis because of our inability to distinguish reliably ERG component waveforms. For the last six subsaturation stimuli ($0.6–2 \times 10^2$ photoisomerizations/rod), distinct a-waves and b-waves were present, and the pSTR and nSTR were no longer detectable. Thus, all inner retina results (pSTR and nSTR) were obtained at stimuli less than 0.1 photoisomerizations/rod, and all other results (a-wave and b-

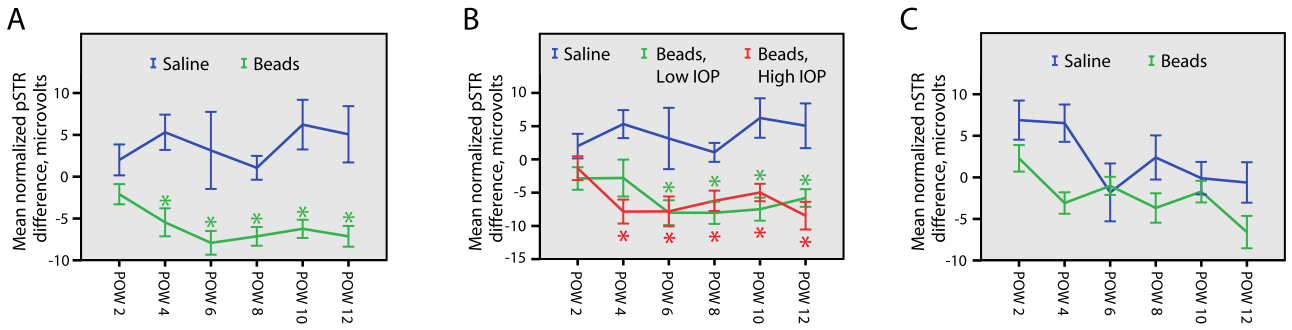

Figure 4. STR analysis. Normalized STR amplitudes are reduced when IOP is elevated. (**A–C**). The normalized pSTR and nSTR difference for each animal was calculated according to Equation 4 (see Materials and Methods). (**A**) Bead-injected eyes have a reduced mean normalized pSTR difference when compared to saline-injected eyes beginning at POW 4 (ANOVA $P < 0.001$, *t*-test, $^* = P < 0.05$). (**B**) The bead-injected animals were split into two equal groups according to the median cumulative IOP difference (see Results). The group with the higher cumulative IOP (Beads, High IOP) had a reduced mean normalized pSTR difference beginning at POW 4, while the group with the lower cumulative IOP (Beads, Low IOP) had a reduced mean normalized pSTR difference beginning at POW6 (*t*-test, $^* = P < 0.05$), suggesting that there is an IOP-dependent effect on normalized pSTR change. (**C**) Bead-injected eyes have a reduced mean normalized nSTR difference (ANOVA $P < 0.05$). However, confirmatory *t*-tests performed at each time point were not statistically significant, suggesting a more mild IOP-dependent effect on the normalized nSTR than for the normalized pSTR. *Error bars* represent one SEM for all panels.

wave) were obtained at stimuli ranging from ($0.6–2 \times 10^2$ photoisomerizations/rod).

Unexpectedly, we observed a statistically significant increase of the mean b-wave response amplitude at all tested light stimuli and at all time points after injection in bead-injected eyes compared to either saline-injected or uninjected eyes (averaged results in Fig. 3E, ANOVA $P < 0.001$). This increase was mild at 2 weeks postinjection, but increased further by 4 weeks postinjection and then remained stable. We found similar changes regardless of the color of beads injected (see Materials and Methods, not shown). We did not detect any alterations of the b-wave latency or tracing shape (not shown). We further assessed the b-wave as an "amplitude difference" determined by subtracting the b-wave amplitude of the uninjected eye from the amplitude of either the bead-injected or saline-injected eye. The mean b-wave amplitude difference then was calculated for all time points and tested light stimuli, and found to be significantly higher for bead-injected animals (averaged results in Fig. 3F, ANOVA $P < 0.001$, *t*-test, $P < 0.05$ for each time point). We also analyzed the b-wave with the "b wave amplitude ratio" (Equation 2), which was found to be higher for bead-injected animals at all time points (Fig. 3G, ANOVA $P < 0.001$, *t*-test, $P < 0.05$ for each time point). Analysis of the b-wave amplitude ratio at individual stimulus strengths yielded the same result at all time points (not shown). To determine if this increase in b-wave response amplitude was due to an increase in photoreceptor light responses, we performed a similar analysis on the a-wave amplitudes. There was no significant increase in the a-wave amplitude of bead-injected eyes compared to saline-injected or uninjected eyes at any tested light stimulus or time point (not shown). Thus, changes in photoreceptor light responses did not appear to explain the increase in b-wave amplitudes.

Next, we evaluated the components of the ERG contributed by the innermost retina, and the pSTR and nSTR. Second-order rod bipolar cells, which generate the b-wave, transfer signals to the post-synaptic third order RGCs and amacrine cells, which generate the dark-adapted STRs. Therefore, in the presence of an increased b-wave and otherwise normal retinal function, we would anticipate a concomitant increase in magnitude of the pSTR and nSTR.[29,31] However, this was not observed, as there was no significant change to either the pSTR or nSTR response amplitude of bead-injected eyes compared to saline-injected or uninjected eyes for either tested light stimulus at any time point (Fig. 3B, see Materials and Methods). One possible explanation for this finding is that diminished inner retinal function prevents adequate transmission of an enhanced bipolar cell signal. As we observed mild RGC loss histologically, we therefore hypothesized that inner retinal cells were dysfunctional.

To test this hypothesis and analyze inner retinal function in the context of increased b-waves, we normalized the pSTR and nSTR amplitudes to the b-wave, and then calculated the normalized pSTR and nSTR difference (Equations 3 and 4). This allowed assessment of the overall gain from bipolar cells to the inner retina. Statistical analysis revealed that the normalized mean pSTR difference was reduced significantly in bead-injected animals at both measured light intensities (averaged results in Fig. 4A, ANOVA $P < 0.001$). Time point analysis showed a reduction in bead-injected animals compared to saline-injected animals beginning at 6 weeks postinjection and continuing at later time points (Fig. 4A, *t*-test, $P < 0.05$). To determine if this normalized reduction was associated with the amount of measured RGC loss, we separated the bead-injected animals into two groups defined as above and below the median level of RGC loss at 12 weeks (mean high RGC loss = 17.7%, mean low RGC loss = 4.6%) and compared both to saline-injected animals. This stratification did not change the time to significance of the normalized pSTR reduction, which still occurred at 6 weeks postinjection in both groups (not shown). Since we had hypothesized that RGC function was abnormal even when cell somas are present, we sought to determine if IOP exposure was a determinant of normalized pSTR reduction. We, therefore, again separated the bead-injected animals into two equal groups, this time according to location above and below the median cumulative IOP difference (mean high IOP = 165.8 mm Hg, mean low IOP = 81.3 mm Hg), and compared both to saline-injected animals. With this stratification, the normalized pSTR difference was reduced sooner in the high cumulative IOP group, with a statistically significant reduction occurring at 4 weeks postinjection. The low cumulative IOP group remained different from saline-injected animals beginning at 6 weeks postinjection (Fig. 4B, *t*-test, $P < 0.05$). Because the group with the higher cumulative IOP exposure had a reduction in the normalized pSTR sooner, this suggests a cumulative IOP-dependent effect on RGC light–evoked electrical activity. Finally, we compared the normalized mean nSTR difference of bead-injected animals to saline-injected animals. Statistical analysis revealed that the normalized mean nSTR difference was reduced significantly in bead-injected animals at both measured light intensities

(averaged results in Fig. 4C, ANOVA $P < 0.05$). However, time point analysis did not yield statistically different results at any time point, suggesting only a weak effect on the normalized nSTR. Stratification of the bead-injected group according to RGC loss or cumulative IOP exposure did not change this result.

Discussion

Injection of Polystyrene Beads Causes a Mild, Chronic Elevation of IOP that Mimics Several Aspects of Human Ocular Hypertension and Early Glaucoma

Our version of the microbead occlusion model successfully recapitulates the critical findings reported by others.[15,16,19] Several components of our version suggested that it represents a good model for human ocular hypertension and its transition to early glaucoma; IOP is mildly and chronically elevated, there are few IOP spikes, and RGC loss is slow, mild, and progressive. Furthermore, because widespread RGC loss is not present, it is likely that we are observing some of the earliest effects of IOP elevation on the eye. Accordingly, our model provides an excellent opportunity to study electrical function in vivo, because the functional changes seen are not likely due to large amounts of cell loss and more likely due to the earliest IOP-induced abnormalities of retinal function.

RGC Loss Does Not Correlate with Total IOP Exposure

We reported an average RGC loss of 7.4% at 6 weeks after bead injection and 11.2% at 12 weeks after bead injection. The only other study conducted in C57Bl/6 mice with a comparable amount of IOP increase reported similar results.[16] This same study did not find a significant correlation between IOP exposure and the amount of RGC loss. Similarly, we did not observe a substantial correlation between cumulative IOP exposure and RGC loss. One explanation for these results is that our ability to monitor mouse IOP is inadequate. As we only measured IOP two times a week, it is possible that we missed spikes in IOP and, therefore, artificially sampled lower IOPs. Since we reported only very mild RGC loss, another explanation is that more animals are required to observe a weak correlation between RGC loss and cumulative IOP exposure. Similarly, it is possible that our experiment end point of 12 weeks is too soon, and longer exposure to IOP is required to observe a correlation with RGC loss. It also is possible that more complex relationships, such as rate of IOP increase or amount of variation, are better correlated with RGC loss. Finally, the very mild IOP we obtained with our model simply may not be high enough to induce large-scale RGC loss in this mouse strain.[17]

Interestingly, we did find that a certain level of average IOP elevation was required to detect RGC loss. Saline-injected control eyes had an average IOP elevation of 1.6 mm Hg across all time points, whereas bead-injected eyes had an average elevation of 4.5 mm Hg. The extremely low level of IOP elevation seen in saline-injected eyes caused no demonstrable difference from uninjected eyes, which supports a relative resistance to IOP-related damage in C57Bl/6 mice.[17] However, with sufficient IOP elevation (as with bead-injected eyes) we did see an effect on RGC loss. This suggested that there is a threshold of resistance to IOP exposure that is crossed with bead injection. Some of the inter-animal variability in RGC loss when correlated with IOP exposure may be explained by unmeasured fluctuations above and below this threshold.

Raw B-Wave Amplitudes Are Increased Very Shortly after IOP-Elevation

We reported that the mean b-wave amplitude increases in bead-injected eyes at all time points, and that the mean b-wave amplitude difference and ratio are increased in bead-injected eyes by 2 weeks postinjection and increase further to a stable level by 4 weeks postinjection (Figs. 3E–G). These results are unexpected as others have reported varying levels of decrease in b-wave and a-wave amplitudes in rat models of ocular hypertension.[21,23,24,26–28] However, the results reported in these studies may be due to the very elevated IOP reported, often as high as 30 mm Hg or greater, which can lead to mild ischemia affecting all layers of the retina, or may be a consequence of inter-species differences between rat and mouse. Since we did not observe a statistically significant concomitant increase in the a-wave amplitude, our data do not imply a global stimulation of retinal electrical activity, but rather suggest that a negatively-contributing component of the b-wave is compromised. Several groups have reported evidence that amacrine cells provide this negative contribution, which may occur through a combination of mechanisms.[29,36–38] Furthermore, multiple lines of evidence suggest that abnormalities in amacrine cell neurotransmitter profiles and function may occur without overt amacrine cell loss in models of experimental glaucoma.[39–41] Consistent with this, we did not observe significant amacrine cell loss, but did observe a subtle but statistically significant decrease in normalized nSTR amplitudes after bead injection (Fig. 4C). Taken together, it is possible that amacrine cell dysfunction underlies our observed increases in the b-wave amplitude.

AII amacrine cells (AIIACs) receive glutamatergic synaptic inputs from depolarizing rod bipolar cells (DBC_Rs), and then make connexin36-mediated electrical synapses (gap junctions) on depolarizing cone bipolar cells (DBC_Cs), which in turn signal to ON-RGCs. In parallel, AIIACs also make chemical (glycinergic) synapses on hyperpolarizing cone bipolar cell axons and OFF-RGCs.[42–45] Therefore, AIIACs serve as a critical relay station for rod-mediated signals. Recent evidence suggests that gap junctions between AIIACs and DBC_Cs likely mediate a portion of the negative component of the scotopic b-wave.[29] Thus, one possible explanation for the observed increase in b-wave amplitude is that perturbation in AIIAC function causes a reduction in their negative contribution to the b-wave. GABAergic amacrine cells also have been implicated as providing negative feedback to the scotopic b-wave, perhaps via their effects on $GABA_A$ receptors.[36–38] Thus, it also is possible that abnormalities in amacrine cell-mediated GABA signaling or changes to $GABA_A$ receptors on bipolar cells result in a loss of negative feedback and an increased b-wave amplitude. A combination of models also is possible, in which global amacrine cell dysfunction occurs. Further studies will be required to distinguish among these possible models.

RGC Electrical Activity Is Reduced in an IOP-Dependent Manner and Precedes Cell Loss

In contrast to RGC loss, we report a correlation between cumulative IOP exposure and the mean normalized pSTR difference (Figs. 4A, 4B). Our normalization of the pSTR is performed according to several assumptions based on our current understanding of retinal circuitry (see text). If our normalization is accurate, these results suggest a decrease in signal gain from bipolar cells to RGCs in dark-adapted retinas. As this decrease occurred as early as 4 weeks after IOP elevation in the group exposed to the highest cumulative IOP, and the amount of RGC loss at the 6-week time point was only 7.4%, this implies that changes to the normalized pSTR occur

in the setting of minimal to no RGC loss and suggests that we are studying RGC function, which is unlikely to be associated with cell death. Thus, in our model, electrical dysfunction of RGCs precedes cell loss. Another group has made a similar conclusion in mice, but the interpretation of these results is complicated by the large amounts of RGC loss observed.[25] Two other reports from a second group also have reported reductions in raw pSTR amplitudes with extreme IOP elevation.[23,24] However, all of these studies report a much higher level of IOP elevation than seen in our model.

Since we are studying normalized full-field ERG recordings and not single-cell patch clamp recordings, we are not able to determine unequivocally if we are observing a reduction in RGC maximum responses, a change in RGC dynamic range, or some other phenomenon that we interpret as a change in RGC function. However, we have indirect evidence that maximum responses are compromised because the effects on the normalized pSTR do not vary with light stimulus strength (not shown). Further studies including the direct analysis of RGC electrical function will be required to distinguish among these possibilities. Taken together, we believe that our data provided evidence for reduced signal gain from bipolar cells to RGCs in dark-adapted retinas, as well as an early susceptibility of RGCs to electrical dysfunction in the setting of even mild IOP elevation. Intriguingly, it is possible that these changes underlie the observation that patients with glaucoma have difficulty with visual performance under dark or dim conditions.[46–49]

Comparison with DBA/2J Strain

Genetic models of elevated IOP also have been studied. The prevailing mouse model is the DBA/2J strain, which displays a variable phenotype, including iris atrophy, pigment dispersion, IOP elevation, and optic nerve degeneration.[50,51] IOP elevation increases by approximately 6 months of age with a further elevation occurring at approximately 8 to 9 months of age, which is highlighted by IOP spikes.[51,52] However, the utility of this strain as a glaucoma model has been questioned because of the large variability and time course of IOP elevation, RGC loss, and axonal degeneration, the presence of degenerative changes in multiple retinal cell types with advanced age, and a significant reduction of outer retinal electrical activity.[52–54] While long-term analyses of microbead-treated eyes have not been reported, with a mild-to-moderate elevation of IOP and minimal IOP spikes, this model of experimental glaucoma seems to overcome several of the difficulties inherent to the DBA/2J strain. In particular, the microbead model seems to be much better suited for studies of retinal function, as its effects consistently do not impact the photoreceptor layer.

Chronic, Mild IOP Elevation Results in Global Inner Retinal Dysfunction

Our model for experimental glaucoma provides an excellent opportunity to observe and characterize retinal behavior in the setting of mild, chronic IOP elevation without significant cell loss. As a consequence we have made several observations that support a model of global inner retina electrical dysfunction involving RGCs and amacrine cells, which begins shortly after IOP elevation and precedes RGC loss. We propose the following sequence of events: by 2 weeks after IOP elevation mild amacrine cell dysfunction leads to an increased b-wave amplitude, by 4 weeks after IOP elevation RGC dysfunction results in a reduced normalized pSTR, and by 6 weeks after IOP elevation minimal RGC loss is present which increases incrementally with time. In parallel, progressive RGC axon compromise occurs as has been reported previously.[19,20]

Our data suggested that IOP elevation may result in the disruption of a much more complex interplay of retinal synapses than previously believed, and a detailed accounting of the timing of changes in synaptic efficacy among RGCs, AII amacrine cells, and rod bipolar cells in response to IOP elevation is critical. If this is true, abnormalities of specific retinal synapses also may explain some of the earliest aspects and variable presentation of visual dysfunction following IOP elevation in humans, occurring in parallel with classic changes to the optic nerve. Consequently, our ability to diagnose early events in human glaucoma may be improved by new tests that quantify these relationships.

Acknowledgments

We thank Philip Lupo for discussion about the statistical analysis.

References

1. Quigley HA, Broman AT. The number of people with glaucoma worldwide in 2010 and 2020. *Br J Ophthalmol*. 2006;90:262–267.
2. Arden GB, Jacobson JJ. A simple grating test for contrast sensitivity: preliminary results indicate value in screening for glaucoma. *Invest Ophthalmol Vis Sci*. 1978;17:23–32.
3. Henson DB, Artes PH, Chauhan BC. Diffuse loss of sensitivity in early glaucoma. *Invest Ophthalmol Vis Sci*. 1999;40:3147–3151.
4. Wilensky JT, Hawkins A. Comparison of contrast sensitivity, visual acuity, and Humphrey visual field testing in patients with glaucoma. *Trans Am Ophthalmol Soc*. 2001;99:213–217, discussion 217–218.
5. Anderson DR. Visual field loss in glaucoma. In: Anderson DR, ed. *Perimetry with and without Automation*. St. Louis: Mosby; 1987:142–159.
6. CNTGSG. The effectiveness of intraocular pressure reduction in the treatment of normal-tension glaucoma. Collaborative Normal-Tension Glaucoma Study Group. *Am J Ophthalmol*. 1998;126:498–505.
7. Gordon MO, Beiser JA, Brandt JD, et al. The Ocular Hypertension Treatment Study: baseline factors that predict the onset of primary open-angle glaucoma. *Arch Ophthalmol*. 2002;120:714–720, discussion 829–730.
8. Leske MC, Heijl A, Hussein M, Bengtsson B, Hyman L, Komaroff E. Factors for glaucoma progression and the effect of treatment: the early manifest glaucoma trial. *Arch Ophthalmol*. 2003;121:48–56.
9. Aihara M, Lindsey JD, Weinreb RN. Experimental mouse ocular hypertension: establishment of the model. *Invest Ophthalmol Vis Sci*. 2003;44:4314–4320.
10. Gross RL, Ji J, Chang P, et al. A mouse model of elevated intraocular pressure: retina and optic nerve findings. *Trans Am Ophthalmol Soc*. 2003;101:163–169, discussion 169–171.
11. Grozdanic SD, Betts DM, Sakaguchi DS, Allbaugh RA, Kwon YH, Kardon RH. Laser-induced mouse model of chronic ocular hypertension. *Invest Ophthalmol Vis Sci*. 2003;44:4337–4346.
12. Ji J, Chang P, Pennesi ME, et al. Effects of elevated intraocular pressure on mouse retinal ganglion cells. *Vision Res*. 2005;45:169–179.
13. Ruiz-Ederra J, Verkman AS. Mouse model of sustained elevation in intraocular pressure produced by episcleral vein occlusion. *Exp Eye Res*. 2006;82:879–884.
14. Urcola JH, Hernandez M, Vecino E. Three experimental glaucoma models in rats: comparison of the effects of intraocular pressure elevation on retinal ganglion cell size and death. *Exp Eye Res*. 2006;83:429–437.

15. Chen H, Wei X, Cho KS, et al. Optic neuropathy due to microbead-induced elevated intraocular pressure in the mouse. *Invest Ophthalmol Vis Sci*. 2011;52:36–44.
16. Cone FE, Gelman SE, Son JL, Pease ME, Quigley HA. Differential susceptibility to experimental glaucoma among 3 mouse strains using bead and viscoelastic injection. *Exp Eye Res*. 2010;91:415–424.
17. Cone FE, Steinhart MR, Oglesby EN, Kalesnykas G, Pease ME, Quigley HA. The effects of anesthesia, mouse strain and age on intraocular pressure and an improved murine model of experimental glaucoma. *Exp Eye Res*. 2012;99C:27–35.
18. Samsel PA, Kisiswa L, Erichsen JT, Cross SD, Morgan JE. A novel method for the induction of experimental glaucoma using magnetic microspheres. *Invest Ophthalmol Vis Sci*. 2011;52:1671–1675.
19. Sappington RM, Carlson BJ, Crish SD, Calkins DJ. The microbead occlusion model: a paradigm for induced ocular hypertension in rats and mice. *Invest Ophthalmol Vis Sci*. 2010;51:207–216.
20. Crish SD, Sappington RM, Inman DM, Horner PJ, Calkins DJ. Distal axonopathy with structural persistence in glaucomatous neurodegeneration. *Proc Natl Acad Sci U S A*. 2010;107:5196–5201.
21. Bayer AU, Danias J, Brodie S, et al. Electroretinographic abnormalities in a rat glaucoma model with chronic elevated intraocular pressure. *Exp Eye Res*. 2001;72:667–677.
22. Ben-Shlomo G, Bakalash S, Lambrou GN, et al. Pattern electroretinography in a rat model of ocular hypertension: functional evidence for early detection of inner retinal damage. *Exp Eye Res*. 2005;81:340–349.
23. Bui BV, Edmunds B, Cioffi GA, Fortune B. The gradient of retinal functional changes during acute intraocular pressure elevation. *Invest Ophthalmol Vis Sci*. 2005;46:202–213.
24. Fortune B, Bui BV, Morrison JC, et al. Selective ganglion cell functional loss in rats with experimental glaucoma. *Invest Ophthalmol Vis Sci*. 2004;45:1854–1862.
25. Holcombe DJ, Lengefeld N, Gole GA, Barnett NL. Selective inner retinal dysfunction precedes ganglion cell loss in a mouse glaucoma model. *Br J Ophthalmol*. 2008;92:683–688.
26. Mittag TW, Danias J, Pohorenec G, et al. Retinal damage after 3 to 4 months of elevated intraocular pressure in a rat glaucoma model. *Invest Ophthalmol Vis Sci*. 2000;41:3451–3459.
27. Moreno MC, Marcos HJ, Oscar Croxatto J, et al. A new experimental model of glaucoma in rats through intracameral injections of hyaluronic acid. *Exp Eye Res*. 2005;81:71–80.
28. Grozdanic SD, Kwon YH, Sakaguchi DS, Kardon RH, Sonea IM. Functional evaluation of retina and optic nerve in the rat model of chronic ocular hypertension. *Exp Eye Res*. 2004;79:75–83.
29. Abd-El-Barr MM, Pennesi ME, Saszik SM, et al. Genetic dissection of rod and cone pathways in the dark-adapted mouse retina. *J Neurophysiol*. 2009;102:1945–1955.
30. Moshiri A, Gonzalez E, Tagawa K, et al. Near complete loss of retinal ganglion cells in the math5/brn3b double knockout elicits severe reductions of other cell types during retinal development. *Dev Biol*. 2008;316:214–227.
31. Saszik SM, Robson JG, Frishman LJ. The scotopic threshold response of the dark-adapted electroretinogram of the mouse. *J Physiol*. 2002;543:899–916.
32. Pease ME, Cone FE, Gelman S, Son JL, Quigley HA. Calibration of the TonoLab tonometer in mice with spontaneous or experimental glaucoma. *Invest Ophthalmol Vis Sci*. 2011;52:858–864.
33. Pang JJ, Wu SM. Morphology and immunoreactivity of retrogradely double-labeled ganglion cells in the mouse retina. *Invest Ophthalmol Vis Sci*. 2011;52:4886–4896.
34. Lyubarsky AL, Daniele LL, Pugh EN Jr. From candelas to photoisomerizations in the mouse eye by rhodopsin bleaching in situ and the light-rearing dependence of the major components of the mouse ERG. *Vision Res*. 2004;44:3235–3251.
35. Chou TH, Kocaoglu OP, Borja D, et al. Postnatal elongation of eye size in DBA/2J mice compared with C57BL/6J mice: in vivo analysis with whole-eye OCT. *Invest Ophthalmol Vis Sci*. 2011;52:3604–3612.
36. Dong CJ, Hare WA. Contribution to the kinetics and amplitude of the electroretinogram b-wave by third-order retinal neurons in the rabbit retina. *Vision Res*. 2000;40:579–589.
37. Kapousta-Bruneau NV. Opposite effects of GABA(A) and GABA(C) receptor antagonists on the b-wave of ERG recorded from the isolated rat retina. *Vision Res*. 2000;40:1653–1665.
38. Moller A, Eysteinsson T. Modulation of the components of the rat dark-adapted electroretinogram by the three subtypes of GABA receptors. *Vis Neurosci*. 2003;20:535–542.
39. Dijk F, van Leeuwen S, Kamphuis W. Differential effects of ischemia/reperfusion on amacrine cell subtype-specific transcript levels in the rat retina. *Brain Res*. 2004;1026:194–204.
40. Gunn DJ, Gole GA, Barnett NL. Specific amacrine cell changes in an induced mouse model of glaucoma. *Clin Experiment Ophthalmol*. 2011;39:555–563.
41. Kielczewski JL, Pease ME, Quigley HA. The effect of experimental glaucoma and optic nerve transection on amacrine cells in the rat retina. *Invest Ophthalmol Vis Sci*. 2005;46:3188–3196.
42. Crooks J, Kolb H. Localization of GABA, glycine, glutamate and tyrosine hydroxylase in the human retina. *J Comp Neurol*. 1992;315:287–302.
43. Pang JJ, Gao F, Wu SM. Light-evoked excitatory and inhibitory synaptic inputs to ON and OFF alpha ganglion cells in the mouse retina. *J Neurosci*. 2003;23:6063–6073.
44. Pourcho RG, Owczarzak MT. Connectivity of glycine immunoreactive amacrine cells in the cat retina. *J Comp Neurol*. 1991;307:549–561.
45. Veruki ML, Hartveit E. AII (Rod) amacrine cells form a network of electrically coupled interneurons in the mammalian retina. *Neuron*. 2002;33:935–946.
46. Ramulu PY, West SK, Munoz B, Jampel HD, Friedman DS. Driving cessation and driving limitation in glaucoma: the Salisbury Eye Evaluation Project. *Ophthalmology*. 2009;116:1846–1853.
47. Nelson P, Aspinall P, O'Brien C. Patients' perception of visual impairment in glaucoma: a pilot study. *Br J Ophthalmol*. 1999;83:546–552.
48. Lee BL, Gutierrez P, Gordon M, et al. The Glaucoma Symptom Scale. A brief index of glaucoma-specific symptoms. *Arch Ophthalmol*. 1998;116:861–866.
49. Janz NK, Wren PA, Lichter PR, et al. The Collaborative Initial Glaucoma Treatment Study: interim quality of life findings after initial medical or surgical treatment of glaucoma. *Ophthalmology*. 2001;108:1954–1965.
50. Chang B, Smith RS, Hawes NL, et al. Interacting loci cause severe iris atrophy and glaucoma in DBA/2J mice. *Nat Genet*. 1999;21:405–409.
51. John SW, Smith RS, Savinova OV, et al. Essential iris atrophy, pigment dispersion, and glaucoma in DBA/2J mice. *Invest Ophthalmol Vis Sci*. 1998;39:951–962.
52. Libby RT, Anderson MG, Pang IH, et al. Inherited glaucoma in DBA/2J mice: pertinent disease features for studying the neurodegeneration. *Vis Neurosci*. 2005;22:637–648.
53. Heiduschka P, Julien S, Schuettauf F, Schnichels S. Loss of retinal function in aged DBA/2J mice – new insights into retinal neurodegeneration. *Exp Eye Res*. 2010;91:779–783.
54. Schuettauf F, Rejdak R, Walski M, et al. Retinal neurodegeneration in the DBA/2J mouse-a model for ocular hypertension. *Acta Neuropathol*. 2004;107:352–358.